Available online at www.sciencedirect.com
SCIENCE DIRECT®
Journal of Molecular Catalysis A: Chemical 235 (2005) 1–11
JOURNAL OF MOLECULAR CATALYSIS A: CHEMICAL
www.elsevier.com/locate/molcata

Nanocrystalline mesoporous Ta_2O_5-based photocatalysts prepared by surfactant-assisted templating sol–gel process for photocatalytic H_2 evolution

Thammanoon Sreethawong, Supachai Ngamsinlapasathian, Yoshikazu Suzuki, Susumu Yoshikawa *

Institute of Advanced Energy, Kyoto University, Uji, Kyoto 611-0011, Japan

Received 24 February 2005; received in revised form 28 March 2005; accepted 29 March 2005
Available online 21 April 2005

Abstract

Nanocrystalline mesoporous Ta_2O_5 photocatalyst was synthesized through a combined sol–gel process with surfactant-assisted templating mechanism under mild conditions. Controlled hydrolysis and condensation of tantalum pentaethoxide modified with acetylacetone in the presence of laurylamine hydrochloride surfactant aqueous solution ultimately yielded nanocrystalline Ta_2O_5 with mesoporous characteristic. The NiO cocatalyst loading at various contents was also performed by single-step sol–gel method, in which nickel precursor was incorporated into the completely hydrolyzed tantalum sol prior to the gelation step. The synthesized photocatalysts were methodically characterized by TG–DTA, XRD, N_2 adsorption–desorption, diffuse reflectance UV–vis spectra, SEM, and TEM analyses. The XRD patterns indicated that the cocatalyst was in a very high dispersion degree on mesoporous Ta_2O_5. N_2 adsorption–desorption isotherms and SEM observation verified that the photocatalysts possessed mesoporous structure. The surface area of the samples from BET method was quite high with very narrow monomodal pore size distribution estimated from BJH method. The photocatalytic performance of the materials was assessed via H_2 evolution from water using methanol as a hole scavenger under UV light irradiation. For unloaded Ta_2O_5 photocatalysts, the sample calcined at 700 °C showed the highest photocatalytic H_2 evolution activity. Moreover, the photocatalytic activity of such the sample was dramatically increased with the cocatalyst loading, exhibiting the optimum loading content at 5 wt.%.

Keywords: Tantalum oxide; Mesoporous material; Surfactant template; Sol–gel; Photocatalysis; Hydrogen evolution

1. Introduction

Photocatalytic water splitting using semiconductors has received much attention, especially for its potential application to direct production of hydrogen (H_2) for clean energy from water utilizing solar light energy. The photoelectrochemical effect of the semiconductors originates from creation of the electrons and holes after absorption of light. Traced to the work of Fujishima and Honda on single-crystal TiO_2 electrodes for water splitting reaction [1], titanium dioxide (TiO_2) has been intensively investigated as photocatalysts in the fields of solar energy conversion, water splitting, and environmental purification [2–6]. Additionally, numerous efforts have been postulated for the fabrication and application of efficient semiconductor manufacture, not only TiO_2 but also other oxide semiconductors.

Tantalum oxide (Ta_2O_5) has attracted increasing interests due to its semiconducting and wide bang gap properties. Ta_2O_5 has been widely used as key material of dynamic random access memory, antireflective coating layer and impedance under high temperature, gas sensor, and capacitor owing to its high dielectric constant, high refractive index, and high chemical stabilization [7,8]. Of late, nanosized and/or nanoporous Ta_2O_5 has also been of technological

* Corresponding author. Tel.: +81 774 38 3504; fax: +81 774 38 3508.
E-mail addresses: thon@iae.kyoto-u.ac.jp (T. Sreethawong), s-yoshi@iae.kyoto-u.ac.jp (S. Yoshikawa).

1381-1169/$ – see front matter © 2005 Elsevier B.V. All rights reserved.
doi:10.1016/j.molcata.2005.03.021

importance because of its photocatalytic performances, particularly for photocatalytic H_2 evolution from water [9–12]. In view of such high application potential of Ta_2O_5 photocatalyst, attempts need to be focused on the synthesis of its mesoporous form, since light harvesting capability and reactant accessibility can be enhanced as a result of multiple scattering and high surface area as well as uniform pore structure.

To date, mesoporous Ta_2O_5 is often prepared by a ligand-assisted templating method involving the complex formation of organic metal precursor with surfactant molecules followed by hydrolyzation-induced precipitation or gelation of the resulting product [10,11,13–15]. Most of the researches utilized very large molecular weight block copolymer, especially Pluronic P-123, or long chain amine surfactant, especially octadecylamine, as the structure-directing agent, which subsequently required severe heat treatment or brought about the difficulty in removal procedure from mesoporous framework. To our knowledge, the application of more simple surfactants for the synthesis of mesoporous Ta_2O_5 has not been extensively examined. Recently, our research group has found a straightforward synthetic method for mesoporous TiO_2 under mild conditions via a combined sol–gel process with surfactant-assisted templating route of laurylamine hydrochloride/tetraisopropyl orthotitanate modified with acetylacetone system [16,17]. The obtained mesoporous TiO_2 possessed considerably higher photocatalytic activity for H_2 evolution reaction compared to some commercially available TiO_2 powders and could be used as an effective based photocatalyst for cocatalyst loading for such the reaction [18].

In this contribution, the combined sol–gel process with surfactant-assisted template was expanded for the synthesis of mesoporous Ta_2O_5 with narrow pore size distribution and high photocatalytic activity, i.e. photocatalytic H_2 evolution as a probe photoreaction. Many characterization techniques, namely TG–DTA, XRD, N_2 adsorption–desorption, diffuse reflectance UV–vis spectra, SEM, and TEM analyses, were performed and explained in details. The effect of NiO cocatalyst loading on the mesoporous Ta_2O_5 was also investigated by single-step sol–gel (SSSG) method to enhance the photocatalytic activity.

2. Experimental

2.1. Materials

Tantalum pentaethoxide (TPE, Hokko Chemical Industry Co., Ltd.), nickel (II) nitrate hexahydrate (Nacalai Tesque, Inc.), laurylamine hydrochloride (LAHC, Tokyo Chemical Industry Co., Ltd), acetylacetone (ACA, Nacalai Tesque, Inc.) and methanol (Nacalai Tesque, Inc.) were used for this study. All chemicals were analytical grade and used without further purification. LAHC was used as a surfactant template behaving as a mesopore-directing agent. ACA serving as a modifying agent was applied to moderate the hydrolysis and condensation processes of titanium precursor. Commercially available Ta_2O_5 powder (orthorhombic phase, surface area $< 0.5\,m^2\,g^{-1}$, particle size 300–1000 nm, Aldrich) was also utilized for comparative study of photocatalytic H_2 evolution.

2.2. Photocatalyst synthesis

The nanocrystalline mesoporous Ta_2O_5 was synthesized via a combined sol–gel process with surfactant-assisted templating mechanism under mild conditions. In typical synthesis, a specified amount of analytical grade ACA was first introduced into TPE with the same mole. The mixed solution was then gently shaken until intimate mixing. Afterwards, 0.1 M LAHC aqueous solution of pH 4.2 was added into the ACA-modified TPE solution, in which the molar ratio of TPE to LAHC was adjusted to a value of 4. The mixed solution was continuously stirred at room temperature for an hour and further aged at 40 °C for a day to attain sol-containing solution as a result of complete hydrolysis of the TPE precursor. Then, the condensation reaction-induced gelation was initiated and formed by placing the sol-containing solution into an oven kept at 80 °C for a week. Subsequently, the gel was dried overnight at 80 °C to eliminate the solvents. The dried sample was calcined at various temperatures for 4 h to remove LAHC template and consequently produce the desired photocatalyst. For single-step sol–gel (SSSG) prepared NiO-loaded samples, a necessary amount of nickel (II) nitrate in methanol for desired loading extents was incorporated into the mixed solution before aging at 40 °C.

2.3. Photocatalyst characterizations

Simultaneous thermogravimetry and differential thermal analysis (TG–DTA, Shimadzu DTG-50) with a heating rate of 10 °C/min in a static air atmosphere was used to study the thermal decomposition behavior of the as-prepared (dried) photocatalysts with α-Al_2O_3 as the reference. Crystalline phases present in the samples were identified by X-ray diffraction (XRD) analysis. A Rigaku Rint-2100 rotating anode XRD system generating monochromated Cu Kα radiation with continuous scanning mode at rate of 2°/min and operating conditions of 40 kV and 40 mA was used to obtain XRD patterns. A nitrogen adsorption system (BEL Japan BELSORP-18 Plus) was employed to measure adsorption–desorption isotherms at liquid nitrogen temperature of 77 K. The Brunauer–Emmett–Teller (BET) approach using adsorption data over the relative pressure ranging from 0.05 to 0.35 was utilized to determine surface area. The Barrett–Joyner–Halenda (BJH) approach was used to yield pore size distribution from desorption data. The samples were degassed at 200 °C for 2 h to remove physisorbed gases prior to the measurement. A Shimadzu UV-2450 UV–vis spectrometer was exploited to record diffuse reflectance spectra of the samples at room temperature with $BaSO_4$ as the reference. The sample morphology was observed by a scanning

electron microscope (SEM, JEOL JSM-6500FE) and a transmission electron microscope (TEM, JEOL JEM-200CX) operated at 5 and 200 kV, respectively.

2.4. Photocatalytic activity measurement

Photocatalytic H_2 evolution reaction was carried out in a closed gas-circulating system. In typical run, a specified amount of photocatalyst (0.2 g) was suspended in an aqueous methanol solution (200 ml of distilled water, 20 ml of CH_3OH) by means of magnetic stirrer within an inner irradiation reactor made of Pyrex glass. A 300 W high-pressure Hg lamp was utilized as the light source. Prior to the reaction, the mixture was left in the dark simultaneously with being thoroughly deaerated by purging with Ar gas for 30 min. Afterwards, the photoreaction system was closed and the reaction was started by exposing to the UV light irradiation. To avoid the heating of the solution during the courses of reaction, water was circulated through a cylindrical Pyrex jacket located around the light source. The gaseous H_2 evolved was periodically collected and analyzed by an on-line gas chromatograph (Shimadzu GC-8A, Molecular sieve 5A, Argon gas), which was connected with a circulation line and equipped with thermal conductivity detector (TCD).

3. Results and discussion

3.1. Photocatalyst characterizations

The thermal decomposition behavior of both the unloaded Ta_2O_5 and 5 wt.% NiO-loaded Ta_2O_5 prepared by the SSSG method, which exhibited the highest photocatalytic activity as explained later, was studied using TG–DTA analysis. The heat treatment process based on the TG–DTA results was also used to calcine all dried samples (xerogel) under appropriate temperatures. Fig. 1 shows the typical TG–DTA curves obtained from the dried gel of unloaded Ta_2O_5. The weight loss until temperature of 200 °C is basically attributable to the removal of water physisorbed at the surface of the photocatalyst. The weight loss in the temperature range of 200–400 °C is due to the burnout of organic LAHC surfactant species contained inside the mesopore of the sample. This is supported by the presence of exothermic peak centered at 386.7 °C in the DTA curve. It is suggested that elimination of the surfactant molecules through oxidation generated the exothermic reaction. Thus, this peak is assigned to the oxidative decomposition of organic surfactant template. The exothermic peak centered at 423.4 °C is mainly resulted from not only the crystallization process of the photocatalysts [19] but also involved with the burnout of a small portion of organic residues as well as the dehydration and evaporation of chemisorbed water [20,21], corresponding to the weight loss in the temperature range of 400–650 °C. The total weight loss from TG curve until 650 °C was 27.95%. This thermal decomposition pattern of the unloaded Ta_2O_5 is relatively the same as

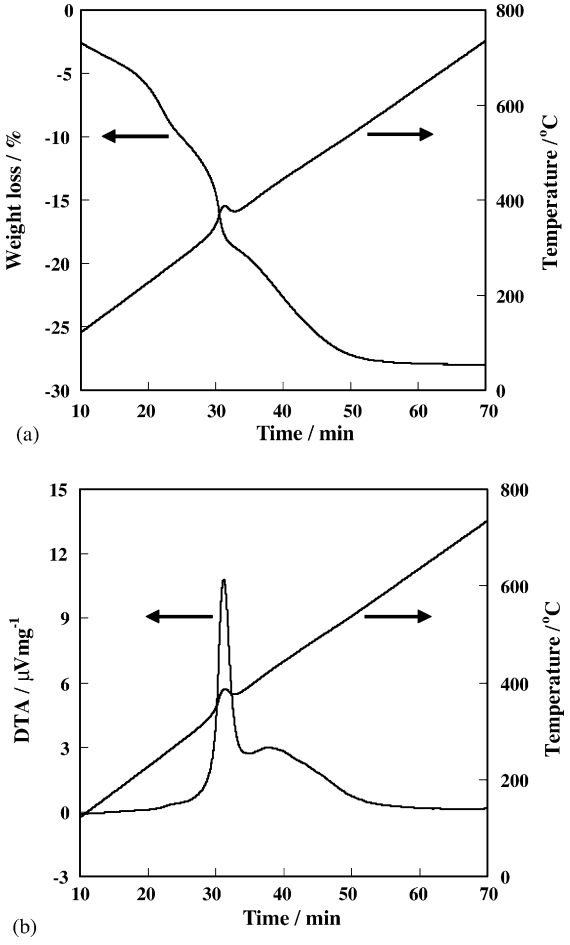

Fig. 1. (a) TG and (b) DTA curves of the as-synthesized (dried) unloaded Ta_2O_5 photocatalyst.

that of the mesoporous TiO_2 case [16,17]. In case of NiO-loaded Ta_2O_5 dried gel, its TG–DTA curves are presented in Fig. 2. The similar weight loss of approximately 4% due to the adsorbed water elimination could be observed. However, from DTA curve, the distinct difference of the thermal decomposition behavior of the NiO-loaded dried gel from the unloaded one regarding to the burnout of surfactant molecules is the presence of two distinguishable exothermic peaks during 200–400 °C. As the nickel precursor was introduced into the completely hydrolyzed tantalum sol during sol–gel preparation in the presence of LAHC surfactant, the nickel molecules were believed to exist between head groups of micellar LAHC and hydrolyzed tantalum sol and subsequently reduce the covalent-bonding interaction between them. The weak exothermic peak centered at 275.6 °C is then resulted from the burnout of a small extent of surfactant molecules, which their interaction with tantalum sol was loosened until being able to be removed by oxidation decomposition at lower temperature. Nevertheless, their large portion underwent the normal burnout characteristic as in the case of the unloaded Ta_2O_5 due to the existence of main exothermic peak centered at 359 °C, which is though slightly lower than that of the unloaded case. The crystallization process combined

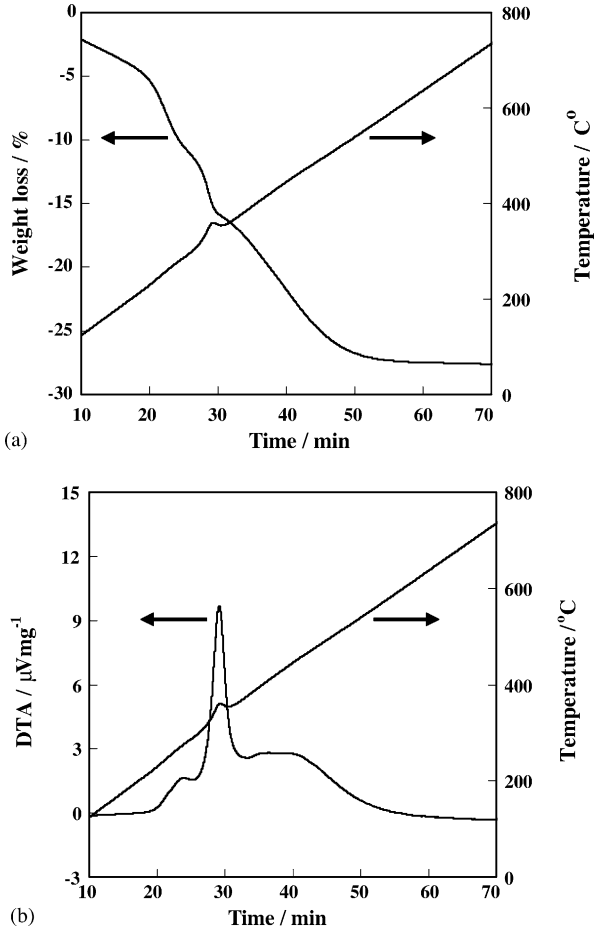

Fig. 2. (a) TG and (b) DTA curves of the as-synthesized (dried) 5 wt.% NiO-loaded Ta_2O_5 photocatalyst.

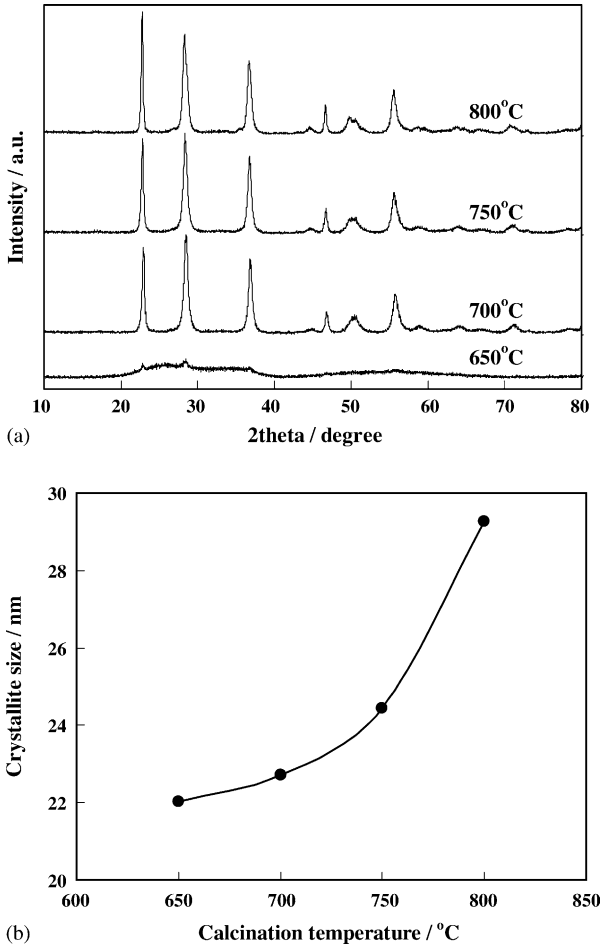

Fig. 3. (a) XRD patterns and (b) crystallite size estimated from line broadening using Sherrer formula of the unloaded Ta_2O_5 photocatalysts calcined at various temperatures for 4 h.

with the elimination of small amount of organic remnants and chemisorbed water could be detected during 400–650 °C with the exothermic peak centered at 419.3 °C, which is also in the same line as the unloaded sample. From TG curve, the total weight loss until 650 °C was 27.52%, almost resembling that obtained from the unloaded Ta_2O_5 as well. For both dried gels, there was no significant weight loss observed beyond 650 °C. Therefore, the results from TG–DTA analysis confirmed that the calcination temperature of 650 °C was adequate for both complete surfactant template removal and photocatalyst crystallization process (but not yet completely crystallized), which was in good agreement with the XRD results. After removal of the surfactant template by calcination process, nickel species were expected to be present as NiO through the mesoporous structure of Ta_2O_5.

XRD analysis is the most useful technique for identification of crystalline structure of the samples. The evolution of the XRD patterns of the unloaded Ta_2O_5 photocatalyst calcined at the desired temperatures ranging from 650 to 800 °C as shown in Fig. 3(a) reveals that the diffractograms were due to the crystallization of amorphous Ta_2O_5 into β-Ta_2O_5 with orthorhombic phase owing to diffraction peaks at 2θ of 22.9°, 28.3°, and 36.7°, which can be filed to (0 0 1), (1 $\bar{1}$ $\bar{1}$ 0), and (1 $\bar{1}$ $\bar{1}$ 1) planes, respectively (JCPDS Card No. 25-0922) [22]. The peak sharpness and intensity increased with temperature, indicating an improvement of crystallinity of the samples accompanied with crystal growth. The crystallite size of the Ta_2O_5 photocatalysts calculated from line broadening of (0 0 1) diffraction peak using Sherrer formula [23] is depicted as a function of calcination temperature in Fig. 3(b). It is obvious that upon calcination at higher temperatures, the crystallite size progressively increased, attesting to the crystal growth of the samples. As the NiO cocatalyst was loaded into the Ta_2O_5 photocatalyst by the SSSG method to enhance the photocatalytic H_2 evolution activity, the presence of the NiO cubic phase was observed by close inspection of XRD patterns in Fig. 4(a) at high loading amount, e.g. at 7 wt.%, according to diffraction peak at 2θ of 43.3° for (2 0 0) plane (JCPDS Card No. 4-0835) [22]. However, the peak intensity was very weak, indicating its high dispersion degree throughout the mesoporous network with small particle size plausibly less than 5 nm due to the minimum sensitivity of XRD analysis. Furthermore, it is worth to note that the crystallite size of the Ta_2O_5 samples from line broadening as illustrated in Fig. 4(b) remained nearly constant up to 4 wt.% NiO load-

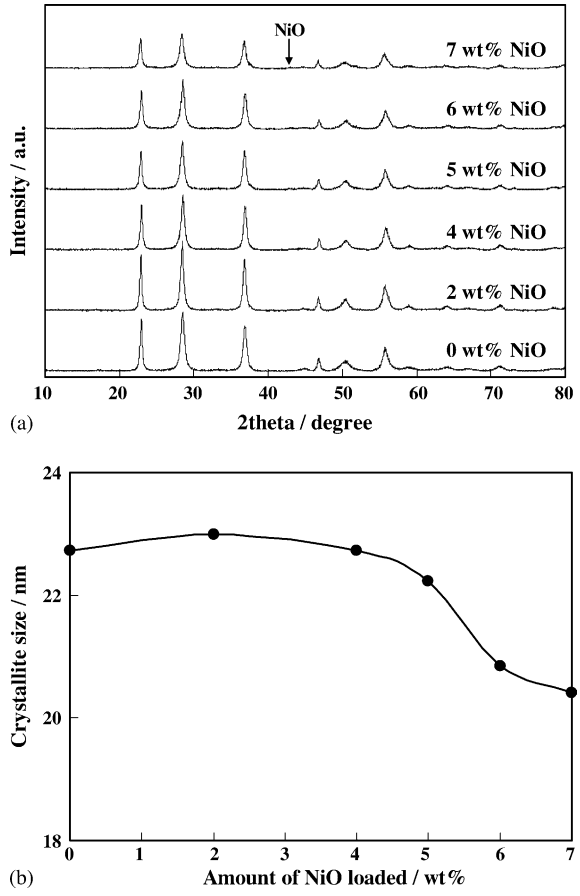

Fig. 4. (a) XRD patterns and (b) crystallite size estimated from line broadening using Sherrer formula of the Ta_2O_5 photocatalysts loaded with various NiO contents and calcined at 700 °C for 4 h.

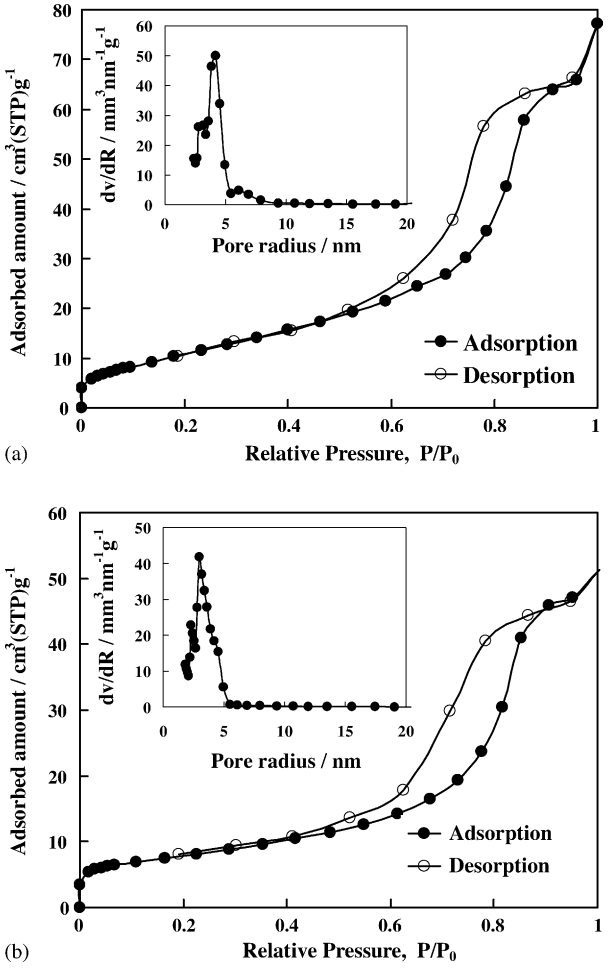

Fig. 5. N_2 adsorption–desorption isotherms and pore size distribution (inset) of (a) the unloaded and (b) the 5 wt.% NiO-loaded mesoporous Ta_2O_5 photocatalysts calcined at 700 °C for 4 h.

ing content and then gradually decreased with increasing the content. This implies that the NiO phase played an inhibitory influence on the Ta_2O_5 crystal growth, but not much significantly.

The N_2 adsorption–desorption isotherms of the unloaded Ta_2O_5 and 5 wt.% NiO-loaded Ta_2O_5 photocatalysts calcined at 700 °C for 4 h are shown in Fig. 5. The shape of the isotherms exhibited the characteristic behavior of the structure of powder, which was composed of an assembly of particles with large open packing. The hysteresis loop in the relative pressure of 0.5–0.9 is typically resulted from wedge-shaped capillaries with a closed edge at the narrow side. According to IUPAC classification [24], this isotherm shape is of type IV as well as shows a marked hysteresis associated with capillary condensation in the mesopore range (2–50 nm). The hysteresis loop in general matches with type H2 pattern. This indicates that the powders contained mesopores in the structure. In addition, the isotherms showed one hysteresis loop, indicating monomodal pore size distribution. The results suggest that a small pore size distribution and uniform pore structure were obtained. The steepness of desorption branch verified the uniformity of the pore diameter with narrow distribution as included in the inset of Fig. 5, which is accredited to the specific synthesis method followed in this proposed route. In many applications, the reagent molecules must be operated across the porous system, as well as the products have to leave the porous materials. Mass transfer process inside the pore depends on pore size and uniformity of pore structure. Inorganic materials with mesopores of between 2 and 50 nm play a role in liquid separations (e.g. cleaning of tap water), catalytic materials, carriers, etc. High surface area implies fine pores, however relatively small pores, such as < 2 nm (micropore region), may become plugged in catalyst preparation, especially if high loading is required.

In the past, the type H2 hysteresis loop was attributed to a difference in mechanism between condensation and evaporation processes occurring in pores with narrow necks and wide bodies, often referred to as ink-bottle pores. This representation can be considered as an over-simplified situation, and it is recommended to take into account the role of network effects [25]. According to the modern point of view [26], the observed hysteresis of the synthesized materials may be the result of two mechanisms: one is an intrinsic property of the phase transition, where a vapor phase may be present at pres-

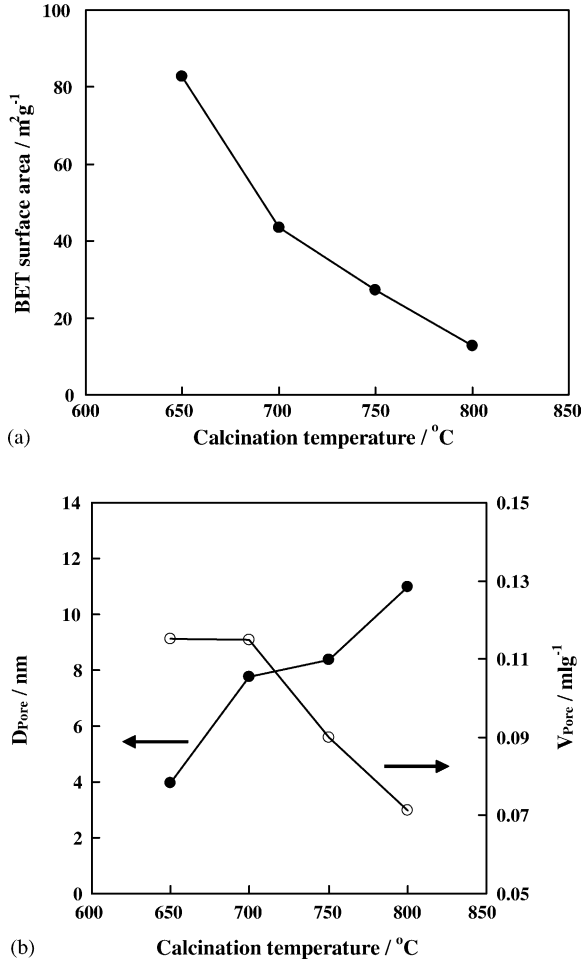

Fig. 6. (a) BET surface area and (b) mean pore diameter and total pore volume of the unloaded mesoporous Ta_2O_5 photocatalysts calcined at various temperatures for 4 h.

sures above the condensation, and a liquid phase below the condensation pressure. This is called the single-pore mechanism. The second mechanism is related to the topology of the pore network, i.e. pore block effects. The structure of the pore network (its connectivity and accessibility), while irrelevant for adsorption, is very critical in the desorption processes. The relative contributions of the single-pore and pore network effects to the hysteresis loop are difficult to ascertain and certainly vary from one solid to another.

The textural properties obtained from N_2 adsorption–desorption measurement, namely BET surface are, mean pore diameter (D_{Pore}), and total pore volume (V_{Pore}), are expressed in Fig. 6 for the unloaded mesoporous Ta_2O_5 calcined at various temperatures and in Fig. 7 for the 5 wt.% NiO-loaded mesoporous Ta_2O_5 calcined at 700 °C for 4 h. From Fig. 6, it is marked that the BET surface area decreased when increasing the calcination temperature from 650 to 800 °C. The apparent decrement in surface area at more severe calcination process can be attributed to pore coalescence upon the crystallization of walls separating mesopores, which is in good accordance with the higher crystallinity and crystal growth from XRD analysis. As a consequence, the increase in mean pore diameter and the decrease in total pore volume were observed, as expected. The mean pore diameter of the samples calcined at various temperatures ranging from 4 to 11 nm confirms that the samples possessed prevalent mesoporous characteristic. When NiO cocatalyst was loaded at various contents up to 7 wt.% by the SSSG method, the BET surface area was gradually reduced as can be seen from Fig. 7(a). The result of such the decrement can be elucidated as a good evidence proving the earlier mentioned hypothesis that the presence of the loaded cocatalyst was along the mesoporous structure after complete surfactant template removal. This subsequently influenced on the decrease in both the mean pore diameter and total pore volume when the loading content was increased because of the higher degree of pore dimension blockage, as illustrated in Fig. 7(b).

Fig. 8 shows the diffuse reflectance UV–vis spectra of the unloaded and NiO-loaded mesoporous Ta_2O_5 as well as pure NiO prepared and calcined at the same conditions as that of mesoporous Ta_2O_5-based photocatalysts for compari-

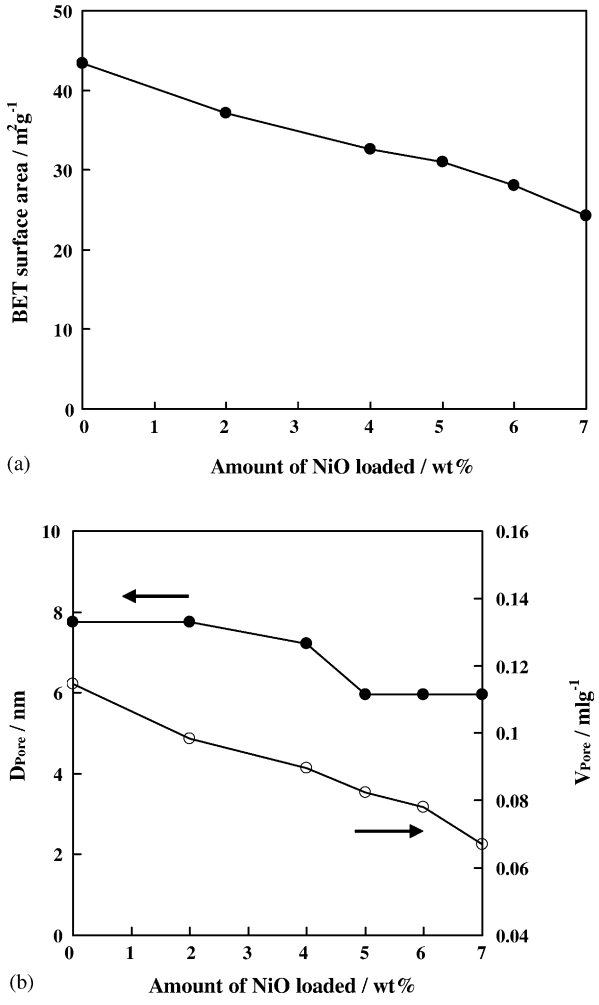

Fig. 7. (a) BET surface area and (b) mean pore diameter and total pore volume of the mesoporous Ta_2O_5 photocatalysts loaded with various NiO contents and calcined at 700 °C for 4 h.

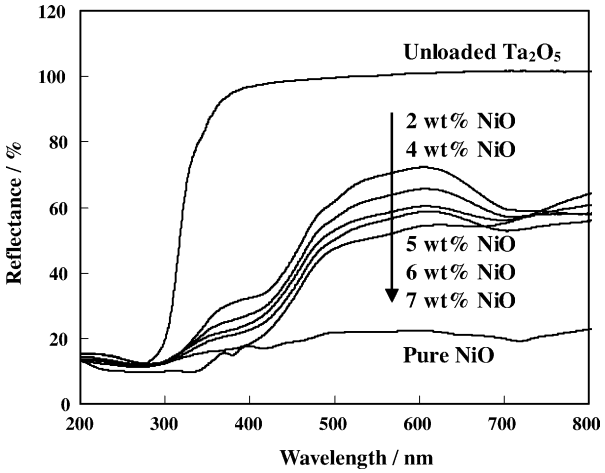

Fig. 8. Diffuse reflectance UV–vis spectra of the unloaded and NiO-loaded mesoporous Ta_2O_5 photocatalysts calcined at 700 °C for 4 h. The spectrum of pure NiO was also included for comparison.

son, which can be used to indicate the electronic environment of the components in the samples during UV–vis excitation. For the unloaded sample, the spectrum revealed the strong absorption band in UV region at approximately 300 nm. This band can be usually indexed to the presence of Ta species as Ta^{5+} due to the electronic excitation of the valence band O 2p electron to the conduction band Ta 5d level. The absorption onset of the spectrum occurred at approximately 315 nm, corresponding to the Ta_2O_5 band gap energy of 4.0 eV [27]. The new absorption bands in the visible region became obvious when the NiO cocatalyst was loaded into the mesoporous Ta_2O_5 as Ni^{2+}. When considering the pure NiO used for comparatively distinguishing the source of absorption in the NiO-loaded mesoporous Ta_2O_5, its spectrum showed the strong absorption through both UV and visible regions due to its dark green color, especially with more intense strong band in UV region at roughly 350 nm. If one compares the spectra of the NiO-loaded mesoporous Ta_2O_5 with that of pure NiO, the absorption onset was noticeably prolonged to longer wavelength with the strong absorption bands owing to both the overlap and interaction between NiO and Ta_2O_5 at around

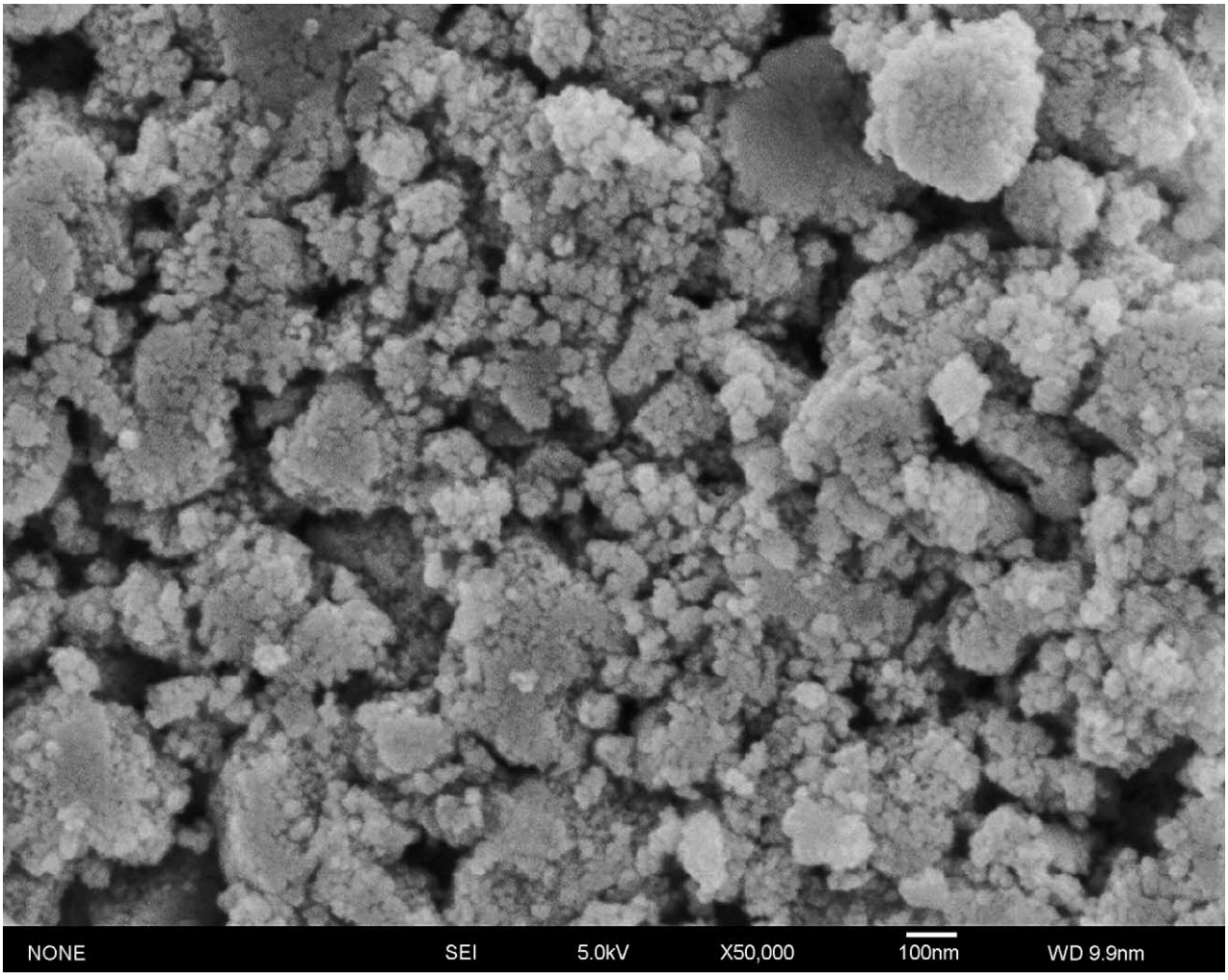

Fig. 9. SEM image of the unloaded mesoporous Ta_2O_5 photocatalyst calcined at 700 °C for 4 h.

350–450 and 600–800 nm as a result of the interdispersion of the two phases originated from the sol–gel process, which well agrees with the CuO/TiO_2 system [28]. In addition, it is evident that the absorption intensity in the visible region gradually increased (the reflectance in opposition decreased), as the cocatalyst loading content was increased.

SEM analysis was used to attain morphological structure of the investigated photocatalysts. The SEM image of the unloaded mesoporous Ta_2O_5 calcined at 700 °C is shown in Fig. 9. It can be perceptible that the particle size was very uniform in the range of 20–25 nm. The aggregation composed of plenty of the nanoparticles could be visibly observed. In order to obtain more insight about the morphology and particle size of the photocatalysts, TEM analysis was also performed. Fig. 10(a) shows the TEM image of the unloaded mesoporous Ta_2O_5 calcined at 700 °C. The formation of Ta_2O_5 aggregates comprising three-dimensional disordered primary nanoparticles could be obviously seen. The particle size of the sample was quite uniform and in the approximate range of 15–25 nm, which is well consistent with the results from both XRD and SEM analyses, signifying that each grain can be considered in average as a single crystallite. Owing to N_2 adsorption–desorption, SEM, and TEM results, the mesoporous structure of Ta_2O_5 particle can be attributed to the pores formed between nanocrystalline Ta_2O_5 particles, which is in the same track as the mesoporous TiO_2 [16,17,29,30]. Similar observation was also perceived in the case of the 5 wt.% NiO-loaded mesoporous Ta_2O_5 sample in Fig. 10(b). However, the presence of NiO particles was not apparent, which is the same as the case of NiO-loaded mesoporous TiO_2 in our previous work [18]. It can be evident that the NiO nanoparticles were deposited on the outer surface and near the outer surface of TiO_2 aggregates in case of the samples prepared by normal incipient wetness impregnation, but not observed for the single-step sol–gel (SSSG) loading method. The existence of most of NiO nanoparticles was expected to be on the surface of mesoporous TiO_2 along mesoporous network, ensuing from the addition of nickel precursor after complete hydrolysis of titanium precursor during the sol–gel process. The analogous consequence was also believed to occur in the NiO-loaded mesoporous Ta_2O_5 samples prepared by the SSSG method.

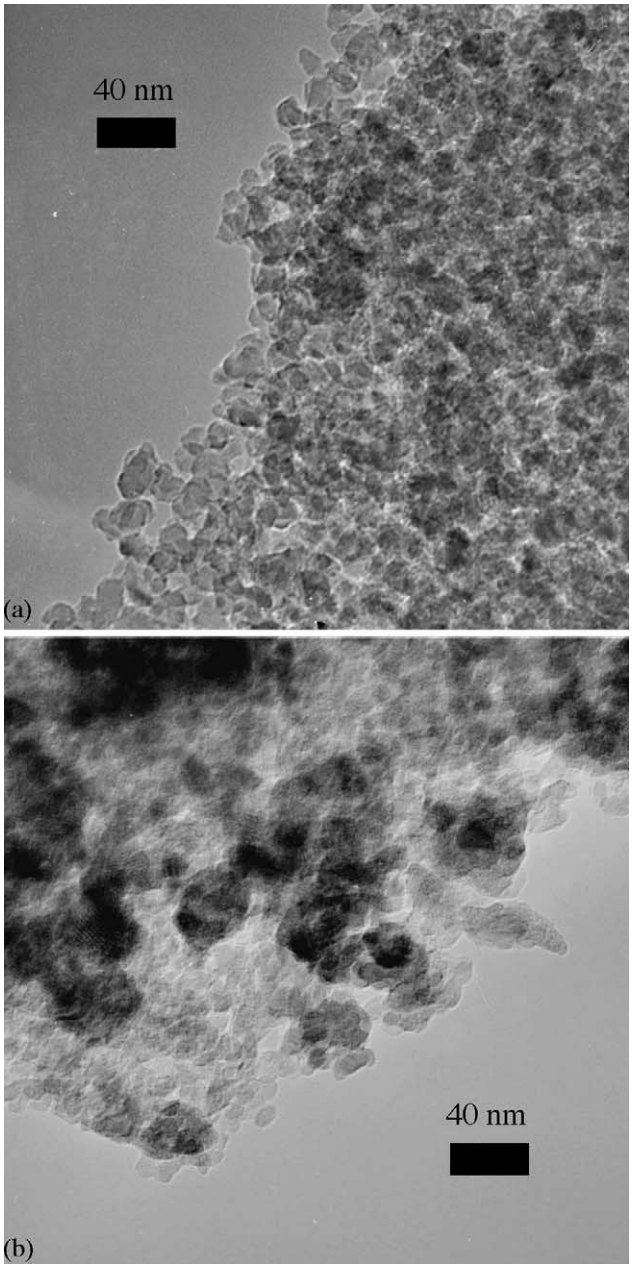

Fig. 10. TEM images of (a) the unloaded and (b) the 5 wt.% NiO-loaded mesoporous Ta_2O_5 photocatalysts calcined at 700 °C for 4 h.

3.2. Photocatalytic activity

The photocatalytic activity for H_2 evolution was determined in a closed gas-circulating system with an on-line gas chromatograph for gaseous H_2 detection. The reaction tests in the absence of either photocatalyst or light irradiation showed insignificantly detectable H_2 gas evolved up to 5 h of reaction time, elucidating that both are definitely indispensable for the photocatalytic H_2 evolution. When both were present in the system, the substantial H_2 evolution could be detected at each interval through the course of reaction.

To study the impact of calcination temperature, the photocatalytic activity was first investigated over the unloaded mesoporous Ta_2O_5 calcined at various temperatures ranging from 650 to 800 °C with 50 °C ramping interval. Fig. 11(a) illustrates the H_2 evolution over these photocatalysts as a function of irradiation time. The amount of evolved H_2 increased almost proportionally to the irradiation time until the end of photocatalytic activity measurement. Thus, the H_2 evolution rate over the entire reaction course could be estimated from these data. The effect of calcination temperature on the H_2 evolution rate is shown in Fig. 11(b). It is obviously seen that the H_2 evolution activity initially increased with increasing the calcination temperature form 650 to 700 °C and then dramatically decreased with further increasing the calcina-

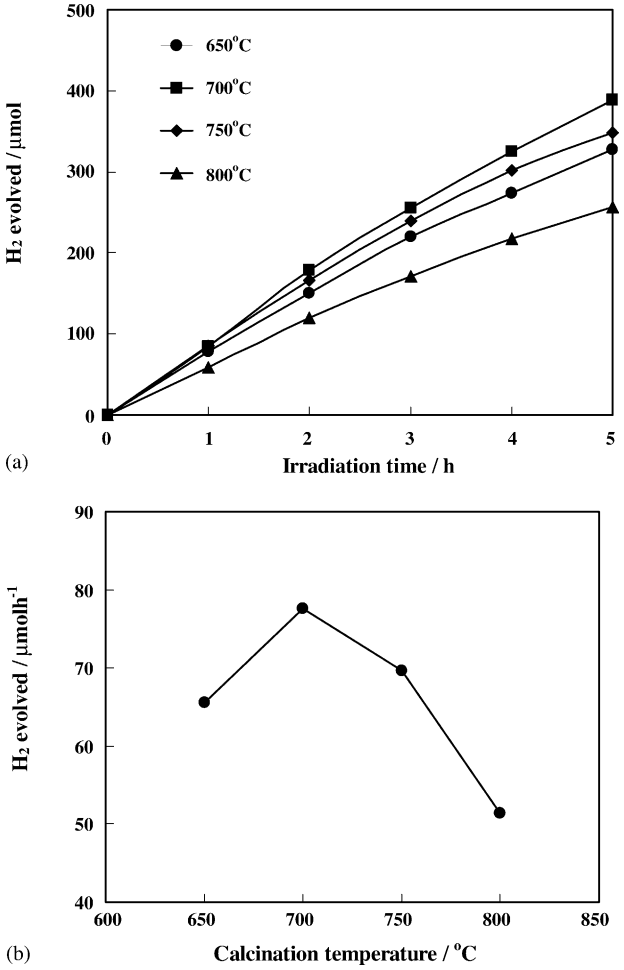

Fig. 11. (a) Time course of H_2 evolution and (b) H_2 evolution rate over the unloaded mesoporous Ta_2O_5 photocatalysts calcined at various temperatures for 4 h.

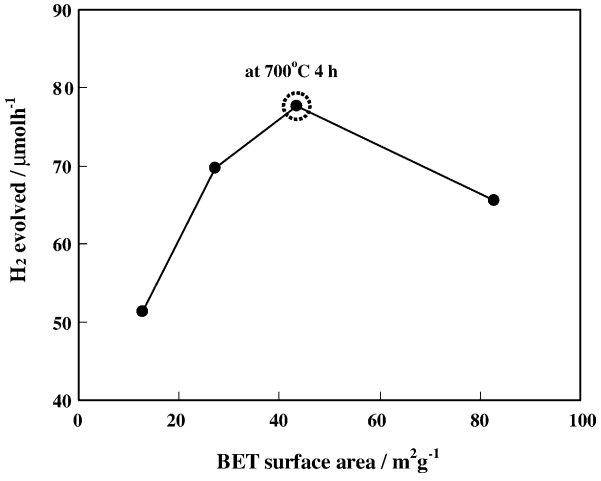

Fig. 12. Dependence of H_2 evolution rate on BET surface area of the unloaded mesoporous Ta_2O_5 photocatalysts calcined at various temperatures for 4 h.

tion temperature to 800 °C. This figures out that the calcination temperature of 700 °C was the optimum point for the unloaded mesoporous Ta_2O_5, exhibiting the highest photocatalytic H_2 evolution activity at the rate of 77.64 μmol h^{-1}. There are many important parameters taken into account to explain the obtained results. In general catalysis, the surface area of sample plays significant role in determining the reaction activity due to the capability of adsorbing reactants on surface active sites for undertaking reaction. Therefore, the H_2 evolution rate is again represented as a function of the BET surface area of the unloaded mesoporous Ta_2O_5, as depicted in Fig. 12. It is found that the BET surface area of 43.43 m^2 g^{-1}, which is the property of the sample calcined at 700 °C (the highest surface area in this study was 82.73 m^2 g^{-1} for the sample calcined at 650 °C), provided the highest H_2 evolution activity. This implies that the surface area was not the critical factor mainly governing the photocatalytic activity. Another essential parameter that has to be considered is the crystallinity. From XRD analysis, it can be seen that despite possessing the highest surface area of the sample calcined at 650 °C, its crystallinity was not yet completely developed. This can be regarded as a major drawback owing to the higher unfavorable e^-/h^+ recombination rate if the lattice defects upon imperfect crystallization are present. On the other hand, at calcination temperature of 700 °C, the crystallinity became almost progressively complete, although the loss of BET surface area in some extent was observed. At this optimum temperature, the increase in the H_2 evolution activity due to the much developed crystallinity may surpass the decrease in the activity due to the lower surface active sites. When the calcination temperature was increased beyond the optimum temperature, i.e. at 750 and 800 °C, the great loss of BET surface area was much more decisive and led to the decrease in the photocatalytic activity. The crystallite size of the samples calcined at these two temperatures was also larger than that at 700 °C. This may accordingly cause the higher probability of bulk recombination of e^-/h^+ pairs upon band gap excitation before reaching the surface active sites.

The photocatalytic H_2 evolution test over the commercially available Aldrich Ta_2O_5 powder was also comparatively performed under identical reaction conditions. The H_2 evolution rate of only 11.74 μmol h^{-1} was obtained, approximately seven folds lower than that of the synthesized mesoporous Ta_2O_5 calcined at the optimum temperature. In comparison, the considerably low photocatalytic activity of the commercial Ta_2O_5 photocatalyst can be reflected to chiefly rise from the lack of mesoporous characteristic due to the absence of hysteresis loop from N_2 adsorption–desorption measurement, leading to very low surface area, as well as the large particle size as confirmed by line broadening of XRD pattern and SEM analysis, leading to relatively high bulk and surface recombination of the photoinduced species. For that reason, the mesoporous structure of Ta_2O_5 photocatalyst, particularly achieved by the investigated surfactant-assisted templating sol–gel process, was verified to be of great importance to attain superior photocatalytic performance.

The photocatalytic H_2 evolution activity of the mesoporous Ta_2O_5 can be drastically enhanced by loading suitable cocatalyst onto the active surface of the photocatalyst. From the reaction mechanism proposed by many researchers [4–6,31,32], after band gap excitation the photoinduced conduction band electrons (e^-) and accompanying valence band holes (h^+) are generated and transferred to surface active sites. The electrons can reduce protons in solution to form H_2 gas. In case of loaded cocatalyst, the electrons will be expeditiously transported and trapped by the cocatalyst and initiate the reduction reaction. This is an effective tool for the prevention of the e^-/h^+ recombination. In this study, NiO was chosen as the investigated cocatalyst, since it can improve the photocatalytic activity of the mesoporous Ta_2O_5 and is much relatively cost-effective cocatalyst compared to noble metals such as Pt. Moreover, the single-step sol–gel (SSSG) method was utilized to prepare the loaded samples because it provided high cocatalyst distribution and also interaction between NiO and Ta_2O_5 for better charge transferring and trapping processes.

The influence of the cocatalyst content was further studied by varying its loading amount up to 7 wt.% during sol–gel preparation and calcining at optimum calcination temperature of 700 °C obtained from the unloaded case. The time course of the H_2 evolution over these photocatalysts is shown in Fig. 13(a). The proportional relationship at all loading contents was also observed. For better clarity to see the effect of cocatalyst loading, the H_2 evolution rate derived from the time course is replotted as a function of loading amount as depicted in Fig. 13(b). It is obvious that the H_2 evolution yield increased with cocatalyst loading, but then decreased when the loading exceeded 5 wt.%. Manifestly, more cocatalyst loading can increase H_2 evolution because of higher amount of active sites. However, the photocatalytic activity of each cocatalyst site declines with more loading amount on mesoporous Ta_2O_5 surface. Therefore, photocatalysts with more than 5 wt.% of the cocatalyst loading cannot further increase the H_2 evolution activity because excess cocatalyst loading can mask the Ta_2O_5 surface, reducing the photoexciting capacity of the mesoporous Ta_2O_5. Hence, there exists an optimum amount of cocatalyst loading at 5 wt.% under the experimental conditions of this study with the increment of photocatalytic H_2 evolution activity up to 182.93 μmol h^{-1}. The optimum cocatalyst loading amount was also found by several researchers, but its value was different from each others depending upon the material preparation methods [10,20]. In case of loaded photocatalysts, although the crystallite size from XRD analysis became smaller at high cocatalyst loading, the surface area decreased with increasing the loading content. Fig. 14 shows the effect of BET surface area of the loaded samples on the H_2 evolution rate. It can be concluded that the balance between the cocatalyst loading content and its corresponding surface area was also vital. At low loading contents compared to the optimum point, the amount of H_2 evolution was lower, even though the surface area was slightly higher. Besides, at too high loading contents, not only less

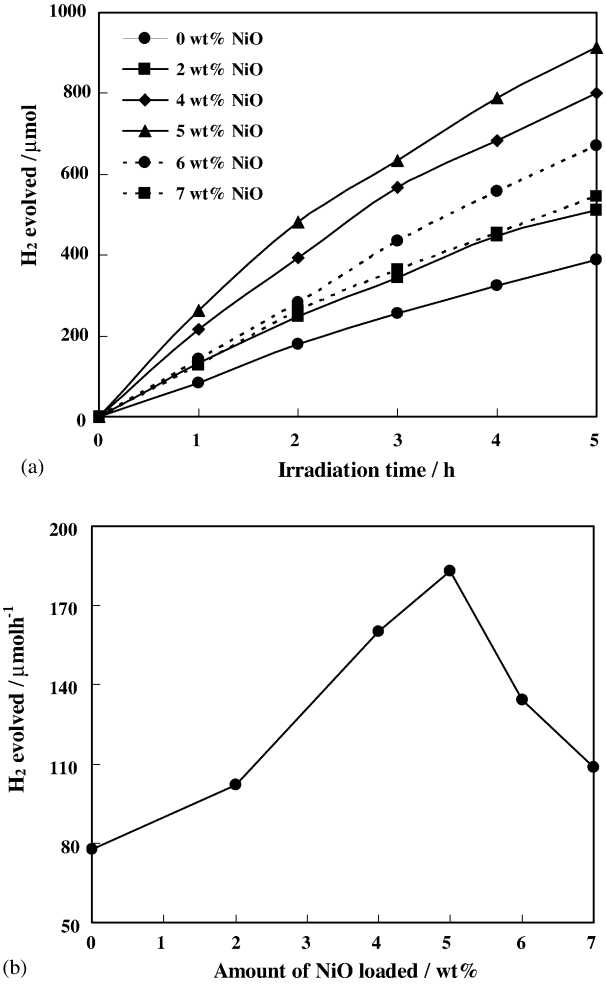

Fig. 13. (a) Time course of H_2 evolution and (b) H_2 evolution rate over the mesoporous Ta_2O_5 photocatalysts loaded with various NiO contents and calcined at 700 °C for 4 h.

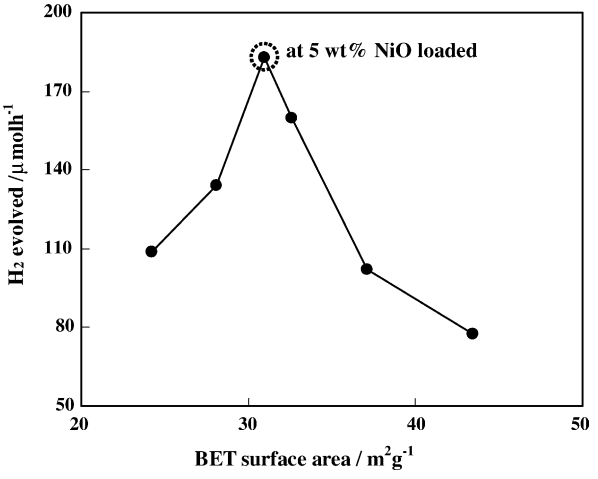

Fig. 14. Dependence of H_2 evolution rate on BET surface area of the mesoporous Ta_2O_5 photocatalysts loaded with various NiO contents and calcined at 700 °C for 4 h.

photoexciting capacity but also less surface active sites for reactant adsorption due to loss of surface area as well as pore diameter and volume played very important role in reducing the photocatalytic activity. At optimum loading content of 5 wt.%, the BET surface area was approximately 31 $m^2\ g^{-1}$, which was sufficient for obtaining the highest photocatalytic H_2 evolution activity.

4. Conclusions

The demonstration for the synthesis under mild conditions of nanocrystalline mesoporous Ta_2O_5 photocatalyst via a surfactant-assisted templating sol–gel route of laurylamine hydrochloride/tantalum pentaethoxide modified with acetylacetone system was reported. The pertinent characterizations revealed that the prepared photocatalyst after appropriate calcination treatment possessed outstanding crystallinity and mesoporous characteristic. The synthesized Ta_2O_5 photocatalyst thermally treated at 700 °C exhibited high photocatalytic activity for H_2 evolution from an aqueous methanol solution. The photocatalytic performance of the mesoporous Ta_2O_5 was considerably improved by NiO cocatalyst loading, which was prepared by the proposed single-step sol–gel method. The optimum loading content was proved to be at 5 wt.%, showing the highest photocatalytic activity under the investigated reaction conditions in this study.

Acknowledgements

This work was financially supported by the Grant-in-aid for Scientific Research from the Ministry of Education, Science, Sports, and Culture, Japan, under the 21COE program and the Nanotechnology Support Project. Grateful acknowledgments are forwarded to (1) Prof. S. Isoda and Prof. H. Kurata and (2) Prof. T. Yoko at Institute for Chemical Research, Kyoto University for their continuous support of the use of TEM and XRD apparatus, respectively.

References

[1] A. Fujishima, K. Honda, Nature 238 (1972) 37.
[2] O. Legrini, E. Oliveros, A.M. Braun, Chem. Rev. 93 (1993) 671.
[3] A. Hagfeldt, M. Gratzel, Chem. Rev. 95 (1995) 49.
[4] M.R. Hoffmann, S.T. Martin, W. Choi, D.W. Bahnemann, Chem. Rev. 95 (1995) 69.
[5] A.L. Linsebigler, G. Lu, J.T. Yates Jr., Chem. Rev. 95 (1995) 735.
[6] A. Mills, S.L. Hunte, J. Photochem, Photobiol. A: Chem. 108 (1997) 1.
[7] R.T. Webb, Electron. Power 2 (1985) 120.
[8] S. Ezhilvalavan, T.Y. Tsentg, J. Mater. Sci. 10 (1999) 9.
[9] H. Kominami, M. Miyakawa, S. Murakami, T. Yasuda, M. Kohno, S. Onoue, Y. Kera, B. Ohtani, Phys. Chem. Chem. Phys. 3 (2001) 2697.
[10] Y. Takahara, J.N. Kondo, T. Takata, D. Lu, K. Domen, Chem. Mater. 13 (2001) 1194.
[11] J.N. Kondo, Y. Takahara, B. Lee, D. Lu, K. Domen, Top. Catal. 19 (2002) 171.
[12] Y. Zhu, F. Yu, Y. Man, Q. Tian, Y. He, N. Wu, J. Solid State Chem. 178 (2005) 224.
[13] D.M. Antonelli, J.Y. Ying, Chem. Mater. 8 (1996) 874.
[14] P. Yang, D. Zhao, D.I. Margolese, B.F. Chmelka, G.D. Stucky, Chem. Mater. 11 (1999) 2813.
[15] B.L. Newalkar, S. Komarneni, H. Katsuki, Mater. Lett. 57 (2002) 444.
[16] T. Sreethawong, Y. Suzuki, S. Yoshikawa, Catal. Commun. 6 (2005) 119.
[17] T. Sreethawong, Y. Suzuki, S. Yoshikawa, J. Solid State Chem. 178 (2005) 329.
[18] T. Sreethawong, Y. Suzuki, S. Yoshikawa, Int. J. Hydrogen Energy, in press, doi:10.1016/j.ijhydene.2004.09.007.
[19] D.C. Hague, M.J. Mayo, J. Am. Ceram. Soc. 77 (1994) 1957.
[20] J.C. Yu, J. Yu, W. Ho, Z. Jiang, L. Zhang, Chem. Mater. 14 (2002) 3808.
[21] J. Yu, H. Yu, B. Cheng, X. Zhao, J.C. Yu, W. Ho, J. Phys. Chem. B 107 (2003) 13871.
[22] J.V. Smith (Ed.), X-ray Powder Data File, American Society for Testing Materials, 1960.
[23] B.D. Cullity, Elements of X-ray Diffraction, Addison–Wesley, Massachusetts, 1978.
[24] F. Rouquerol, J. Rouquerol, K. Sing, Adsorption by Powders and Porous Solids: Principles, Methodology and Applications, Academic Press, San Diego, 1999.
[25] K.S.W. Sing, D.H. Everett, R.A.W. Haul, L. Moscou, R.A. Pierott, J. Rouquerol, T. Siemieniewska, Pure Appl. Chem. 57 (1985) 603.
[26] C.K. Lee, S.L. Lee, Heterogen. Chem. Rev. 3 (1996) 269.
[27] K. Sayama, H. Arakawa, J. Photochem. Photobiol. A: Chem. 77 (1994) 243.
[28] X. Bokhimi, A. Morales, O. Novaro, T. López, O. Chimal, M. Asomoza, R. Gómez, Chem. Mater. 9 (1997) 2616.
[29] J.C. Yu, J. Yu, W. Ho, L. Zhang, Chem. Commun. 19 (2001) 1942.
[30] J. Yu, J.C. Yu, M.K.P. Lueng, W. Ho, B. Cheng, X. Zhao, J. Zhao, J. Catal. 217 (2003) 69.
[31] N. Serpone, E. Pelizzetti, Photocatalysis: Fundamentals and Applications, Wiley, New York, 1989.
[32] N. Serpone, R.F. Khairutdinov, Semiconductor Nanoclusters, Physical, Chemical, and Catalytic Aspects, Elsevier, Amsterdam, 1997.